



Magnets for accelerator, an accelerated view

Presented by P. Fessia
TE-MS-C-MNC



Acknowledgments

Thanks to the colleagues that have provided support and material to prepare this seminar. In particular, A. Ballarino, F. Cerutti, P. Ferracin, M. Karppinen, E. Todesco, D. Tommasini, T. Zickler and many others.




References

- Fifth General Accelerator Physics Course, CAS proceedings, University of Jyväskylä, Finland, September 1992, CERN Yellow Report 94-01
- International Conference on Magnet Technology, Conference proceedings
- Iron Dominated Electromagnets, J. T. Tanabe, World Scientific Publishing, 2005
- Magnetic Field for Transporting Charged Beams, G. Parzen, BNL publication, 1976
- Magnete, G Schnell, Thiemig Verlag, 1973 (German)
- Electromagnetic Design and mathematical Optimization Methods in Magnet Technology, S. Russenschuck, e-book, 2005
- CAS proceedings, Magnetic measurements and alignment, Montreux, Switzerland, March 1992, CERN Yellow Report 92-05
- CAS proceedings, Measurement and alignment of accelerator and detector magnets, Anacapri, Italy, April 1997, CERN Yellow Report 98-05
- Physik der Teilchenbeschleuniger und Synchrotronstrahlungsquellen, K. Wille, Teubner Verlag, 1996
- CAS proceedings, Magnets, Bruges, Belgium, June 2009, CERN Yellow Report 2010-004

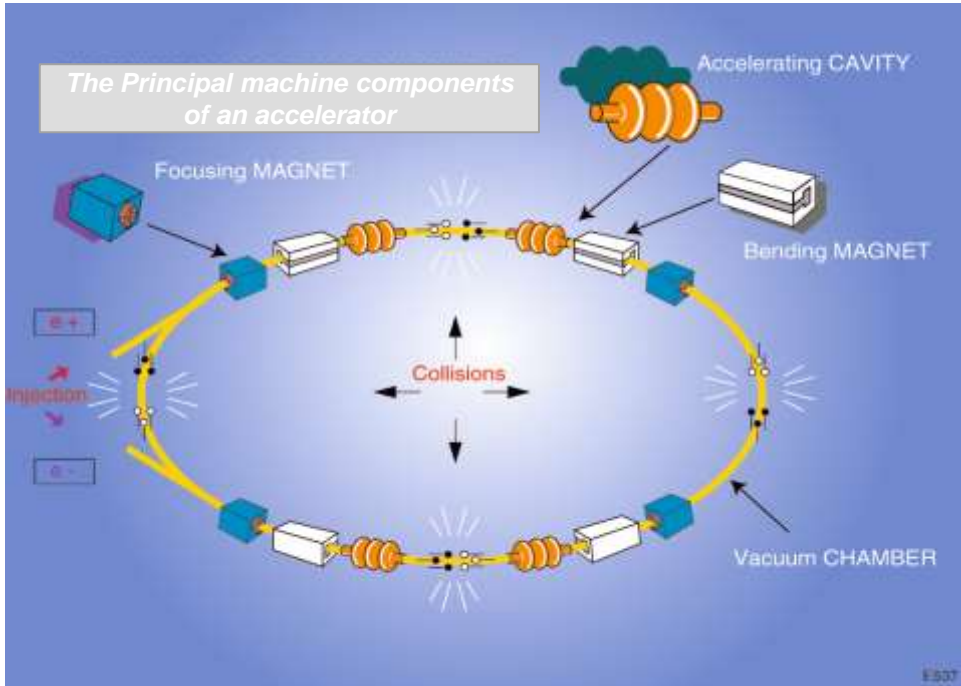


Outline

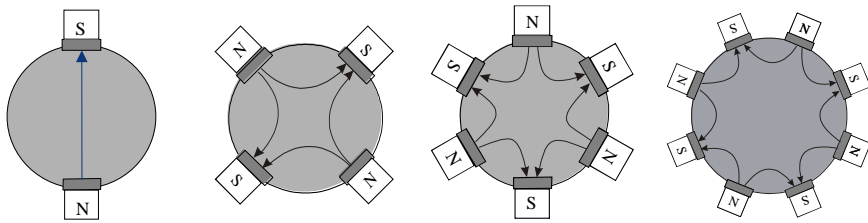
- Introduction to magnets for accelerators
 - Normal conducting magnets or iron dominated magnets
 - Field
 - Forces
 - Cooling
 - Construction
 - An example of technological issue: the insulation radiation resistance
 - Superconducting materials
 - Superconducting magnets
 - Field, forces and structures
 - An example of technological issue: the insulation
-  Superconducting magnet construction

INTRODUCTION

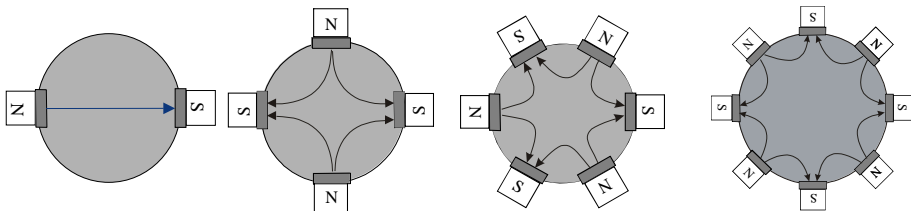




Magnet types : field harmonics



NORMAL : vertical field on mid-plane



SKEW : horizontal field on mid-plane



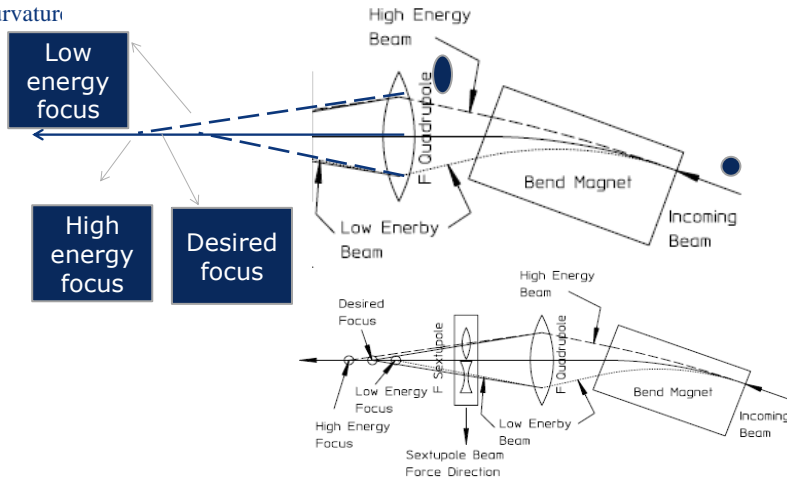
Field type: shape and function I

	<p>Dipoles=Bending magnets: bend the beam along the set path</p>		
	<p>Quadrupoles=Focus sing magnets: move the particles back to the centre of the aperture</p>		

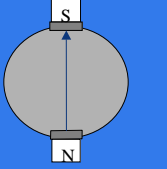

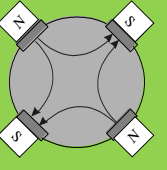

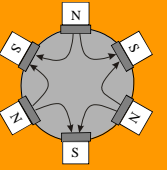
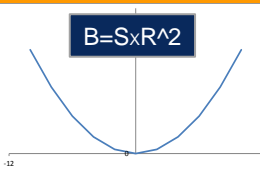
Why sextupole ?

$$B\rho = \frac{1}{qc} \sqrt{T^2 + 2TE_0}$$

- q = charge in Coulombs
- c = the speed of light in m/sec
- T = beam energy
- E0 = the particle rest mass energy
- ρ = radius of curvature



Field type: shape and function II

	<p>Dipoles=Bending magnets: bend the beam along the set path</p>		
	<p>Quadrupoles=Focus sing magnets: move the particles back to the centre of the aperture</p>		
	<p>Sextupole=correct for the chromatic aberration due to dispersion in a dipole caused by the momentum spread in the beam.</p>		

NORMAL CONDUCTING MAGNET OR IRON DOMINATED MAGNETS



Field type: shape and function III

	<p>Dipoles=Bending magnets: bend the beam along the set path</p>	<p>$B=K$</p>	<p>Flux Lines $\psi = \frac{1}{2} B_0 x$</p> <p>Field Directional $\psi = \frac{1}{2} B_0 x$</p> <p>From Equipotential $\psi = \frac{1}{2} B_0 x$</p>
	<p>Quadrupoles=Focus sing magnets: move the particles back to the centre of the aperture</p>	<p>$B=G \times R$</p>	<p>Flux Lines $\psi = \frac{1}{2} G x^2 - \frac{1}{2} G y^2$</p> <p>From Equipotential $\psi = \frac{1}{2} G x^2 - \frac{1}{2} G y^2$</p> <p>From Equipotential $\psi = \frac{1}{2} G x^2 - \frac{1}{2} G y^2$</p> <p>From Equipotential $\psi = \frac{1}{2} G x^2 - \frac{1}{2} G y^2$</p>
	<p>Sextupole=correct for the chromatic aberration due to dispersion in a dipole caused by the momentum spread in the beam.</p>	<p>$B=S \times R^2$</p>	<p>Flux Lines $\psi = \frac{1}{6} S x^3 - \frac{1}{2} S x y^2 + \frac{1}{6} S y^3$</p> <p>From Equipotential $\psi = \frac{1}{6} S x^3 - \frac{1}{2} S x y^2 + \frac{1}{6} S y^3$</p> <p>From Equipotential $\psi = \frac{1}{6} S x^3 - \frac{1}{2} S x y^2 + \frac{1}{6} S y^3$</p>

Shaping the field

$$(\vec{B}_2 - \vec{B}_1) \cdot \vec{n} = 0$$

$$(\vec{H}_2 - \vec{H}_1) \times \vec{n} = \frac{4\pi}{c} \vec{K}$$

$$\vec{B}_2 \cdot \vec{n} = \vec{B}_1 \cdot \vec{n}$$

$$\frac{\vec{B}_2}{\mu_2} \times \vec{n} = \frac{\vec{B}_1}{\mu_1} \times \vec{n} \rightarrow \vec{B}_2 \times \vec{n} = \frac{\mu_2}{\mu_1} \vec{B}_1 \times \vec{n}$$

$$B_2 \cos \alpha_2 = B_1 \cos \alpha_1$$

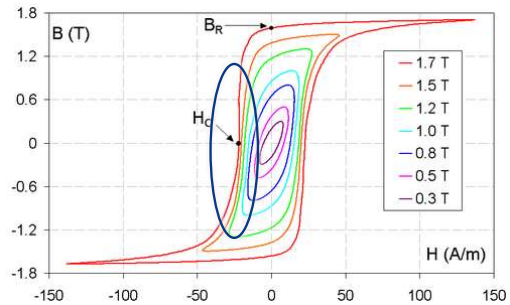
$$B_2 \sin \alpha_2 = \frac{\mu_2}{\mu_1} B_1 \sin \alpha_1$$

$$\tan \alpha_2 = \frac{\mu_2}{\mu_1} \tan \alpha_1$$

$$\tan \alpha_2 = \frac{\mu_{r2} \mu_0}{\mu_{r1} \mu_0} \tan \alpha_1$$

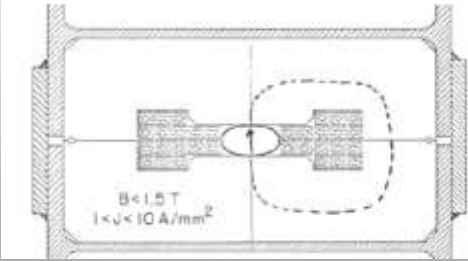
$$\tan \alpha_2 = \frac{1}{\mu_{r1}} \tan \alpha_1$$

$$\mu_{r1} \gg 1 \rightarrow \alpha_2 \sim \frac{\pi}{2}$$



Therefore the flux line (to which the \vec{B} is tangent point by point) is perpendicular to the shape of the interface between a material with high μ_r and the air independently of the shape of the flux lines in that materials

Creating the field->you need coil



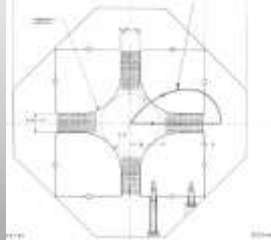
$$\oint H \cdot dl = NI$$

$$NI(\text{ampere turns}) = \oint \frac{B}{\mu} \cdot dl = \frac{Bg^{\text{air}}}{\mu_0} + \frac{B\ell^{\text{iron}}}{\mu_0} \left(\frac{\mu_0}{\mu_{\text{iron}}} \right)$$

$\left(\frac{\mu_0}{\mu_{\text{iron}}} \right) \frac{g}{\ell} \gg 1$

$NI \propto \text{gap}$
 $P \propto$
 $NI^2 \propto$
 gap^2

$$NI(\text{ampere turns}) = \frac{B \text{ (weber/m}^2\text{)} g(\text{meter})}{\mu_0 = 4\pi \times 10^{-7} \text{ (meter/ampmeter)}}$$



$$\oint H \cdot dl = NI$$

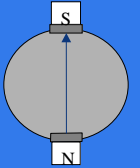
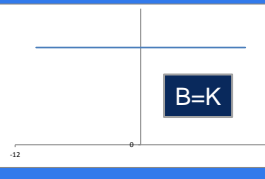
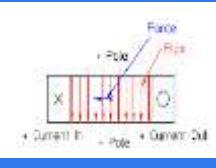
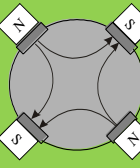
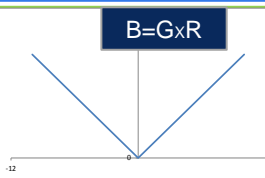
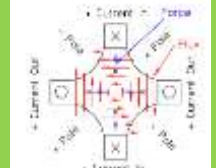
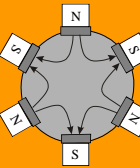
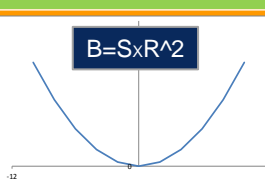
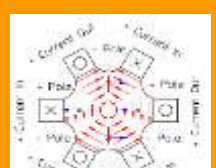
$$NI = \oint H \cdot dl = \int \frac{B(r)}{\mu^2} dr + [\text{iron path}] + [\text{path } \perp \text{ to the field}]$$

$$= \int_0^a Kr dr = \frac{Ka^2}{2}$$

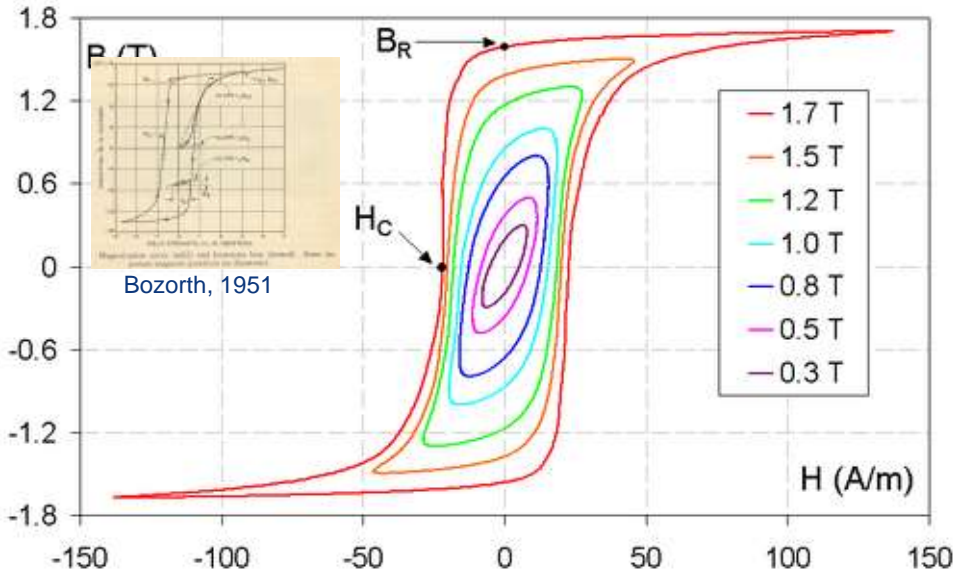
But, since $Ka = B_{\text{pole}} \ell_p$

$$\frac{NI}{\text{pole}} = \frac{B_{\text{pole}} \ell_p (\text{weber/m}^2) \times a(\text{m})^2}{2\mu_0 = 2(4\pi \times 10^{-7})}$$

Field type: shape and function, real magnet

	<p>Dipoles=Bending magnets: bend the beam along the set path</p>	 <p style="text-align: center;">B=K</p>	
	<p>Quadrupoles=Focusing magnets: move the particles back to the centre of the aperture</p>	 <p style="text-align: center;">B=GxR</p>	
	<p>Sextupole=correct for the chromatic aberration due to dispersion in a dipole caused by the momentum spread in the beam.</p>	 <p style="text-align: center;">B=SxR^2</p>	

But iron saturates ,.....

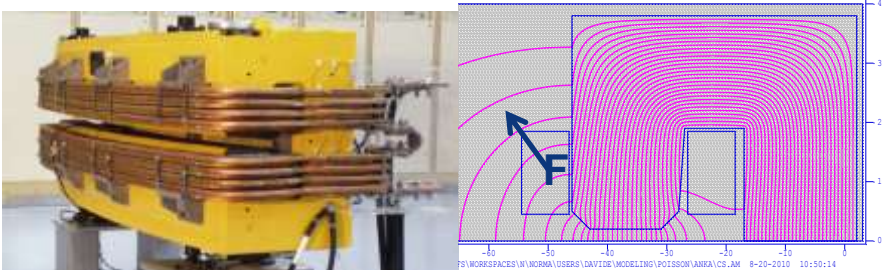


For iron, above 1.5-2 T any increase of magnetic field costs a lot of magnetomotive force

Effect of interaction field with the coil current:

On a conductor immersed in magnetic field

$$\mathbf{F} = I \cdot \mathbf{L} \times \mathbf{B}$$



Example for the Anka dipole:
 On a the external coil side with N=40 turns, I= 700A, L~2.2 m
 in an average field of B= 0.25 T



$$F = 40 \cdot 700 \cdot 2.2 \cdot 0.25 = 15400 \text{ N} = 0.015 \text{ MN} \sim 1.5 \text{ tons}_f$$

$$0.007 \text{ MN/m}$$

Losses and heat removal

In a coil of cross section S , total current I , per unit of length l ,

$$P/l [W/m] = \frac{\rho}{S} \cdot I^2$$

$$\rho_{cu} = 1.72 \cdot (1 + 0.0039 \cdot (T - 20)) \cdot 10^{-8} \Omega \cdot m$$

In the yoke we have losses due to:

- hysteresis: up to 1.5 T we can use the Steinmetz law

$$P [W/kg] = \eta \cdot f \cdot B^{1.6}$$

with $\eta = 0.01 \div 0.1$, about 0.02 for silicon steel

- eddy currents: for silicon iron, an approximate formula is

$$P [W/kg] = 0.05 \cdot (d_{lam} \cdot \frac{f}{10} \cdot B_{av})^2$$

where d_{lam} is the lamination thickness in mm



To increase the temperature of 1 kg of water by 1 degree C we need 1 kcal = 1/4.186 kJ

$$Q [l/min] = 14.3 \cdot \frac{P [kW]}{\Delta T}$$

To efficiently cool a pipe you need the fluid velocity be greater than zero on the wall, i.e. the flow being moderately turbulent (Reynolds > 2000):

$$R_e = \frac{d \cdot v}{\nu} \sim 1400 \cdot d [mm] \cdot v [m/s] \text{ for water at } \sim 40^\circ C$$

Small pipes need high velocity, however attention to erosion ($v > 3 m/s$)!

As cooling pipes in magnets can be considered smooth, a good approximation of the pressure drop ΔP as a function of the cooling pipe length L , the cooling flow Q and the pipe hole diameter d is derived from the Blasius law, giving:

$$\Delta P [bar] = 60 \cdot L [m] \cdot \frac{Q [l/min]^{1.75}}{d [mm]^{4.75}}$$

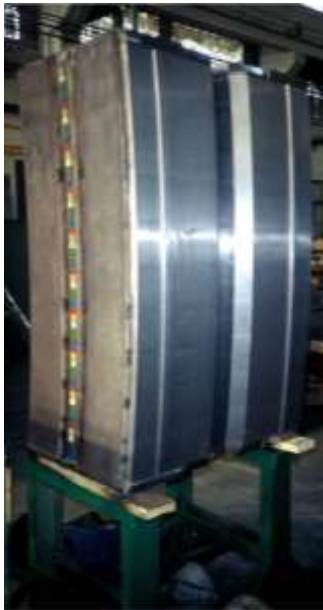
Normal conducting magnet construction



Coil production



Iron yoke production

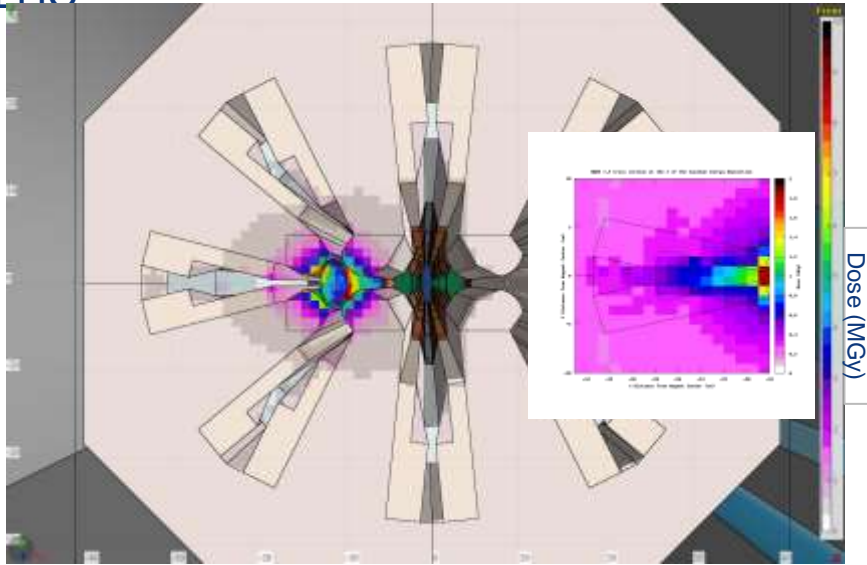




*An example of technological issue:
the insulation radiation resistance*



Dose on a normal conducting magnet in the LHC



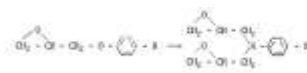
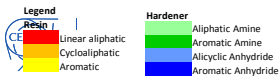
Normalization: $1.15 \cdot 10^{16}$ p (30-50 fb⁻¹).
Computations with E 6.5 TeV relaxed collimator settings

Different epoxy

Resins	Hardeners	Additives	Composition (p.p.)	Mix Temp (°C)	Viscosity (cPs)	Service life (mn)	Fig	Dose for 50% flex. (MGy)	Dose Range (MGy)	
EDBAH	MA						5.4	1.4	1 - 3	
EDBAH	MA	BDMA	100-105-0.2	80	45	>180	5.1	1.6		
BECP	MA						5.4	2.5		
BECP	MA	BDMA	100-110-0.2	80	40	>180	5.1	2.3	1 - 6	
ECC	MA		100-72	80	20	>240	5.5	1.8		
YCO	MA	BDMA	100-160-05	60	20	>180	5.4	3.7		
DADD	MA		100-65	80	180	>240	5.4	5.5	1 - 2	
DGEBA + DGDPP	TETA		100-20-12	25			5.21	1.3		
DGEBA	TETA	DBP	83-9-17	50	500	few	5.22	1.2		
DGEBA	DADPPS		100-35	130	60	180	4.2	5.1	5 - 15	
DGEBA + DGDPP	MDA		100-20-30	80			5.21	8.2		
DGEBA	MDA		100-27	80	100	50	5.9	13.0		
DGEBA	MPDA		100-14.5	65	200	30	5.7	23.5	23	
DGEBA	AT		100-40	100	150	30	5.26	45.2		45
DGEBA	DOSA	BDMA	100-130-1	80	70	120	5.2	4.2		
DGEBA	NMA	BDMA	100-80-1	80	80	120	5.2	5.9		
DGEBA	MA		100-100	60	69	>1440	5.23	7.1	5 - 15	
DGEBA	MA	BDMA					5.1	12.0		
DGEBA	MA	BDMA + Po. Gl.	100-100-0.1-10	60	65	300	5.23	12.1		
DGEBA	MA		100-70	120	26	180	5.2	13.0	20 - 40	
DGPP	DADPPS		100-28	130			5.6	8.2		
DGPP	MA		100-135	120			5.3	13.0		
EDIC	MDA		100-20	80		40	5.9	10.0	5 - 15	
TGTFE	DADPPS		100-34	125	>20000		5.6	12.1		
TGTFE	MA	BDMA	100-100-0.2	125	>15000		5.3	10.6		
EPN	DADPPS		100-35	100		30	5.6	23.5	20 - 40	
EPN	MDA		100-29	100		35	5.10	37.2		
EPN	NMA	BDMA	100-76-1	80		40	5.40	13.0		
EPN	MA	BDMA	100-105-0.5	80		100	5.3+5.35	15.0	10 - 20	
EPN	NMA	BDMA	100-85-1	100		80	5.10	20.6		
TGMD	DADPPS		100-40	80		50	5.6	20.6		
TGMD	MA	BDMA	100-136-0.5	60		30	5.3	11.4	10 - 25	
TGMD	NMA	BDMA	100-110-1	80	500	20	5.8	18.0		
TGPAP	NMA		100-137	80	<20		5.8	23.5		
DGA	NMA		100-20	25		120-420	5.7	23.5	20 - 30	
DGA	NMA		100-115	25	5 - 20	30-5760	5.8	28.6		

Aromatic
 Cycloaliphatic
 Linear Aliphatic

- Aliphatic amine hardener
→ poor radio-resistance
- Aromatic amine hardener
>
- Anhydride hardener
H: Too high local concentration of benzene may induce steric hindrance
- Good radio-resistance even if Cl (tendence to capture n_{th})
- Novolac: HIGH Radio-resistance
• Large nb of epoxy groups
→ Density, acidity
- Glycidyl-amine: HIGH R.-resistance
• Quaternary carbon
→ weakness
• Ether group (R-epi-ly)
→ weakness
• amine



Filler contribution

Resins	Hardeners	Additives	Filler	Composition (p.p.)	Fig	Dose for 50% flex. (MGy)	Dose Range (MGy)
DGEBA	MDA		Papier	100-27-200	5.14	1.3	1 - 2
DGEBA	MDA		Silice	100-27-200	5.14	10	10 - 15
DGEBA	MDA		Silice	100-27-200	5.18	11.4	
DGEBA	MDA		Silice (5 micron)	100-27-20	5.16	14.8	
DGEBA	MDA		Silice (20 micron)	100-27-20	5.16	14.8	
DGEBA	MDA		Silice (40 micron)	100-27-20	5.16	14.6	
DGEBA	MDA		Silice (40 micron)	100-27-200	5.17	12.1	
DGEBA	HPA	BDMA	Silice (40 micron)	100-80-2-200	5.17	<10	<10
DGEBA	MDA		Aérosil + Sulphate de Barium	100-27-2-150	5.14	15.8	15
DGEBA	MDA		Magnésie	100-27-120	5.14	18	18
DGEBA	MDA		Graphite	100-27-60	4.6	26.8	
DGEBA	MDA		Graphite	100-27-60	5.14	30.5	25 - 30
DGEBA	MDA		Alumine	100-27-220	4.7	23.5	
DGEBA	MDA		Alumine	100-27-220	5.14	51.7	20 - 50
DGEBA	MDA		Alumine	100-27-100	5.15	20.6	
DGEBA	MDA		Alumine	100-27-220	5.15	42.5	
DGEBA	MDA		Fibre de verre	100-27-50	5.19	82	80 - 100
DGEBA	MDA		Fibre de verre	100-27-60	5.18	100	
EPN	MDA		Fibre de verre	100-29-50	5.19	>100	>100
TGMD	MDA		Fibre de silice	100-41-50	5.20	>100	>100
TGMD	DADPS		Fibre de silice	100-40-50	5.20	>100	

Legend Resin

- Linear aliphatic
- Cycloaliphatic
- Aromatic

Hardener

- Aliphatic Amine
- Aromatic Amine
- Alicyclic Anhydride
- Aromatic Anhydride

2 Categories of fillers:

1. Powder fillers
2. Glass/Silice fibers ($C_6H_{10}O_9/n$)

Paper [cellulose $C_6H_{10}O_9/n$]
 → Strong decrease of radio-resistance

The bigger the powder, the more radio-resistant

Hardener choice not influenced by filler

High r.-resistance for Graphite and Alumina

The more fillers, the more radio-resistant

Best Radio-Resistant materials are obtain with Glass/Silice (influence of boron) fibers and aromatic resins (Novolac and glycidyl-amine)

CERN 98-01-A/E

Material: Epoxy resin: TIS No R 422
 Type: MY 745 (50) + EPN 1138 (50) + CV 223 (20) + HY 905 (120) + DY 973 (0.5)

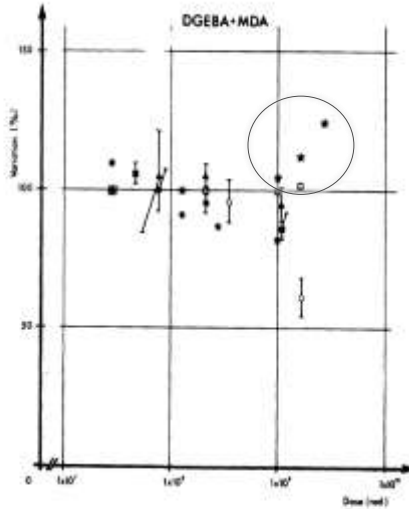
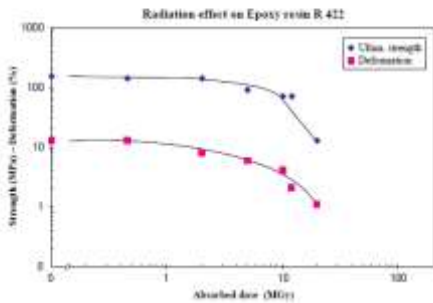
Supplier: Ciba-Geigy U.L. 74: sans LOE

Remarks: used for the 2SR dipoles

Radiation test results according to IEC Standard 544 (and ISO 178)

Dose rate (kGy/h)	Dose (MGy)	Ultim. strength (MPa)	Deformation r. (%)	Modulus (GPa)
0	0	153±1	13.1±1.5	3.90±0.03
0.1	0.5	142±1	12.9±0.3	3.90±0.02
0.1	2.0	140±1	7.8±0.3	3.90±0.02
180	5	93±2	8.1±0.3	4.00±0.03
180	10	72±1	4.2±0.2	4.10±0.04
0.5	12	71±0	2.1±0.2	3.7±0.1
180	20	15±1	1.1±0.1	3.40±0.04

Radiation index (RI) = 0.9 if strength is the critical property
 Radiation index (RI) = 0.6 if deformation is the critical property

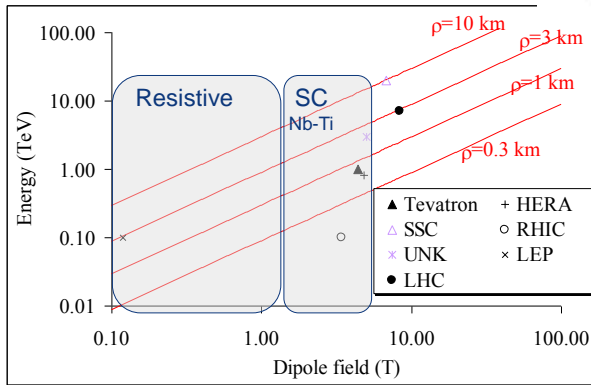
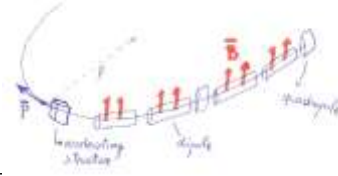


Modifications des propriétés mécaniques de DGEBA+MDA en fonction des doses absorbées

- 1 - Résistance à la flexion: 1.7 kg/cm²
- 2 - Résistance à la traction: 32 kg/cm²
- 3 - Module d'élasticité: 322 kg/cm²
- 4 - Allongement à la rupture: mm
- 5 - Résistance au choc: 25 kg.m²/cm²
- 6 - Dureté: 80 Shore D
- 7 - Absorption d'eau -25°C, 4 jours: 0.6 %
- 8 - Point de fléchissement à la chaleur: 126 °C

The limits of NC magnet application

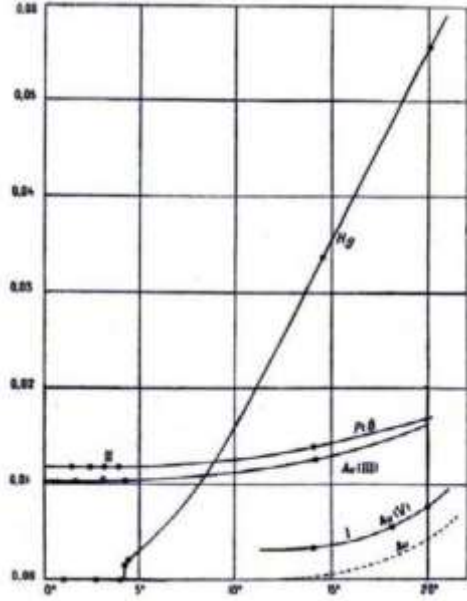
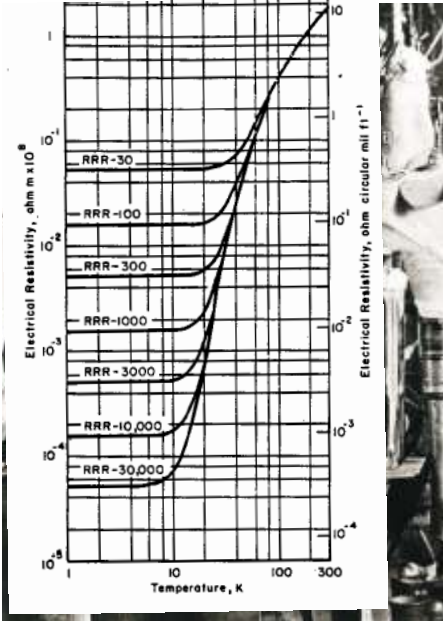
$$B\rho = \frac{1}{qc} \sqrt{T^2 + 2TE_0}$$



SUPERCONDUCTING MATERIALS



Superconductivity

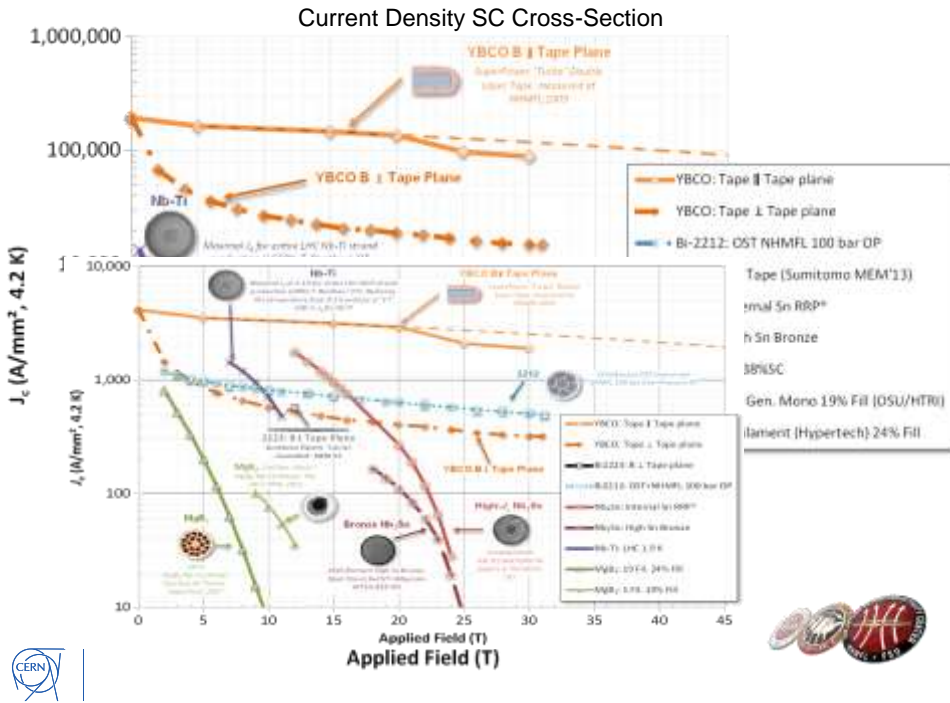
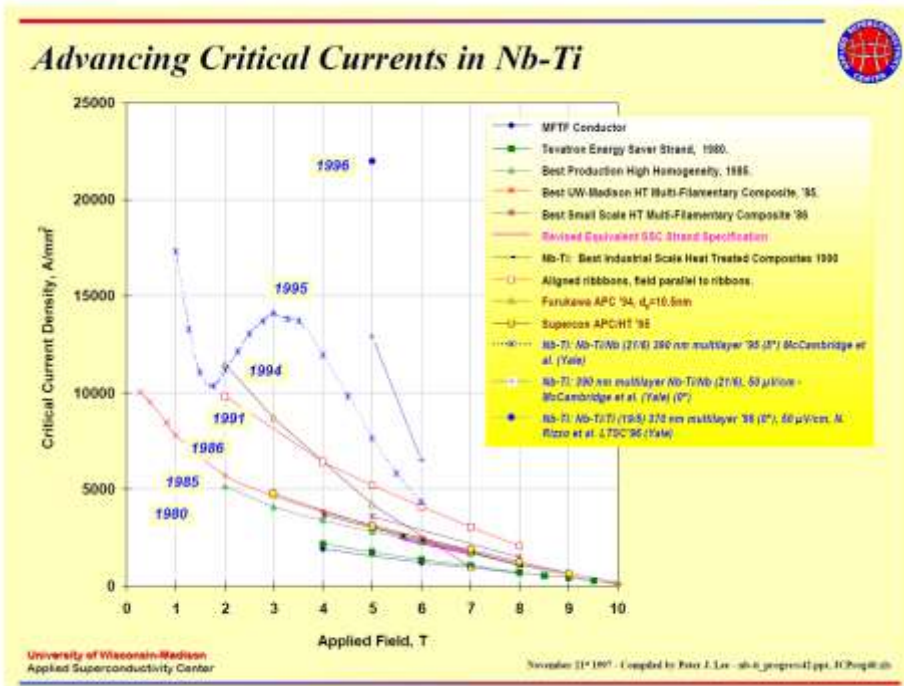


Superconductivity at 100

In the 100 years since the discovery of superconductivity, progress has come in fits and starts. The graph below shows the history of superconductivity and the progress of research in this area. The graph shows the history of superconductivity and the progress of research in this area. The graph shows the history of superconductivity and the progress of research in this area.

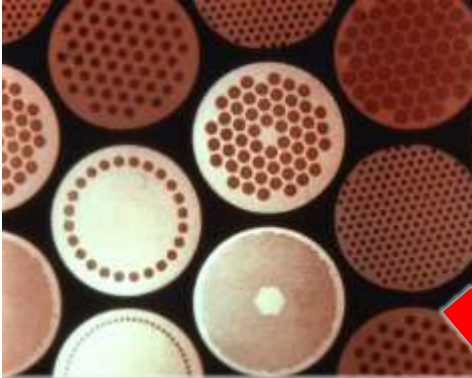
The figure is a timeline of superconductivity research from 1900 to 2010. The y-axis is 'Superconducting transition temperature, T_c (K)' ranging from 0 to 140. The x-axis is 'Year' ranging from 1900 to 2010. Key events are marked with icons and text boxes:

- 1900**: Heike Kamerlingh Onnes discovers superconductivity in mercury.
- 1911**: Heike Kamerlingh Onnes discovers superconductivity in lead.
- 1915**: Heike Kamerlingh Onnes discovers superconductivity in tin.
- 1933**: Walter Brattain and Robert Schrieffer discover the BCS theory of superconductivity.
- 1938**: Heike Kamerlingh Onnes and Fritz London discover the London equations.
- 1950**: Heike Kamerlingh Onnes and Fritz London discover the London equations.
- 1957**: Heike Kamerlingh Onnes and Fritz London discover the London equations.
- 1961**: Heike Kamerlingh Onnes and Fritz London discover the London equations.
- 1962**: Heike Kamerlingh Onnes and Fritz London discover the London equations.
- 1963**: Heike Kamerlingh Onnes and Fritz London discover the London equations.
- 1964**: Heike Kamerlingh Onnes and Fritz London discover the London equations.
- 1965**: Heike Kamerlingh Onnes and Fritz London discover the London equations.
- 1966**: Heike Kamerlingh Onnes and Fritz London discover the London equations.
- 1967**: Heike Kamerlingh Onnes and Fritz London discover the London equations.
- 1968**: Heike Kamerlingh Onnes and Fritz London discover the London equations.
- 1969**: Heike Kamerlingh Onnes and Fritz London discover the London equations.
- 1970**: Heike Kamerlingh Onnes and Fritz London discover the London equations.
- 1971**: Heike Kamerlingh Onnes and Fritz London discover the London equations.
- 1972**: Heike Kamerlingh Onnes and Fritz London discover the London equations.
- 1973**: Heike Kamerlingh Onnes and Fritz London discover the London equations.
- 1974**: Heike Kamerlingh Onnes and Fritz London discover the London equations.
- 1975**: Heike Kamerlingh Onnes and Fritz London discover the London equations.
- 1976**: Heike Kamerlingh Onnes and Fritz London discover the London equations.
- 1977**: Heike Kamerlingh Onnes and Fritz London discover the London equations.
- 1978**: Heike Kamerlingh Onnes and Fritz London discover the London equations.
- 1979**: Heike Kamerlingh Onnes and Fritz London discover the London equations.
- 1980**: Heike Kamerlingh Onnes and Fritz London discover the London equations.
- 1981**: Heike Kamerlingh Onnes and Fritz London discover the London equations.
- 1982**: Heike Kamerlingh Onnes and Fritz London discover the London equations.
- 1983**: Heike Kamerlingh Onnes and Fritz London discover the London equations.
- 1984**: Heike Kamerlingh Onnes and Fritz London discover the London equations.
- 1985**: Heike Kamerlingh Onnes and Fritz London discover the London equations.
- 1986**: Heike Kamerlingh Onnes and Fritz London discover the London equations.
- 1987**: Heike Kamerlingh Onnes and Fritz London discover the London equations.
- 1988**: Heike Kamerlingh Onnes and Fritz London discover the London equations.
- 1989**: Heike Kamerlingh Onnes and Fritz London discover the London equations.
- 1990**: Heike Kamerlingh Onnes and Fritz London discover the London equations.
- 1991**: Heike Kamerlingh Onnes and Fritz London discover the London equations.
- 1992**: Heike Kamerlingh Onnes and Fritz London discover the London equations.
- 1993**: Heike Kamerlingh Onnes and Fritz London discover the London equations.
- 1994**: Heike Kamerlingh Onnes and Fritz London discover the London equations.
- 1995**: Heike Kamerlingh Onnes and Fritz London discover the London equations.
- 1996**: Heike Kamerlingh Onnes and Fritz London discover the London equations.
- 1997**: Heike Kamerlingh Onnes and Fritz London discover the London equations.
- 1998**: Heike Kamerlingh Onnes and Fritz London discover the London equations.
- 1999**: Heike Kamerlingh Onnes and Fritz London discover the London equations.
- 2000**: Heike Kamerlingh Onnes and Fritz London discover the London equations.
- 2001**: Heike Kamerlingh Onnes and Fritz London discover the London equations.
- 2002**: Heike Kamerlingh Onnes and Fritz London discover the London equations.
- 2003**: Heike Kamerlingh Onnes and Fritz London discover the London equations.
- 2004**: Heike Kamerlingh Onnes and Fritz London discover the London equations.
- 2005**: Heike Kamerlingh Onnes and Fritz London discover the London equations.
- 2006**: Heike Kamerlingh Onnes and Fritz London discover the London equations.
- 2007**: Heike Kamerlingh Onnes and Fritz London discover the London equations.
- 2008**: Heike Kamerlingh Onnes and Fritz London discover the London equations.
- 2009**: Heike Kamerlingh Onnes and Fritz London discover the London equations.
- 2010**: Heike Kamerlingh Onnes and Fritz London discover the London equations.



Superconductor material, but under which conductor shape

for 5 to 10kA, we need 20 to 40
wires in parallel



- a single 5 μ m filament of Nb-Ti in 6T carries 50mA
- a composite wire of fine filaments typically has 5,000 to 10,000 filaments, so it carries 250A to 500A

$$v = \frac{LI}{t} = \frac{2E}{It}$$



The main reason why Rutherford cable succeeded where others failed was that it could be compacted to a high density (88 - 94%) without damaging the wires. Furthermore it can be rolled to a good dimensional accuracy (~ 10mm).
Note the 'keystone angle', which enables the cables to be stacked closely round a circular aperture

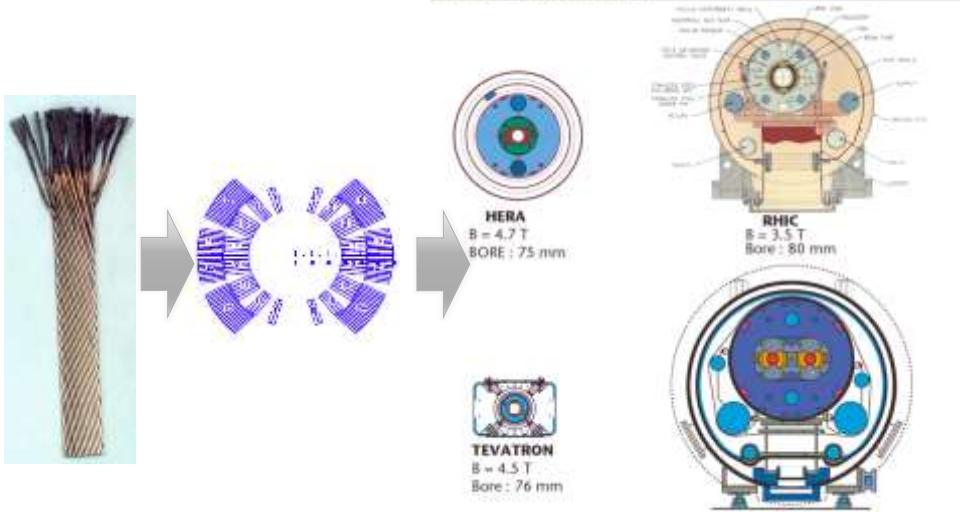


SUPERCONDUCTING MAGNETS



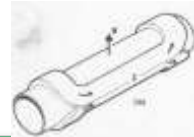
How we can use the SC cable ?

DIPOLE MAGNETS



Remark: the field here is higher of ferromagnetic material therefore the iron is pushed out where the field is lower and closes the flux lines

GENERATION OF MAGNETIC FIELDS: FIELD OF A WINDING



$|B| = \frac{I\mu_0}{2\pi\rho}$

$I \rightarrow j\rho d\rho d\theta$

$$B = -4 \frac{j\mu_0}{2\pi} \int_0^\alpha \int_r^{r+w} \frac{\cos\theta}{\rho} \rho d\rho d\theta = -\frac{2j\mu_0}{\pi} w \sin\alpha$$

$B \propto$ current density
 $B \propto$ coil width w
 B is independent of the aperture r

$|B| = \frac{I\mu_0}{2\pi\rho}$

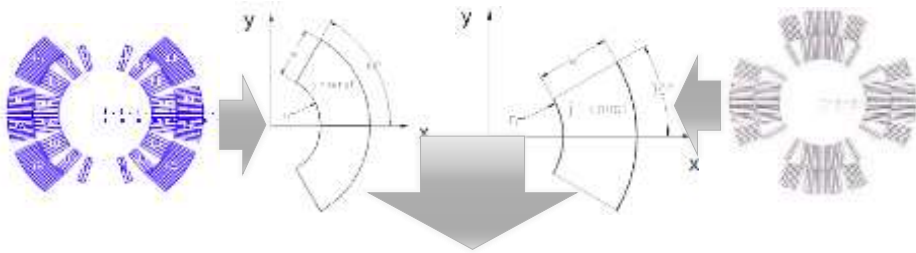
$I \rightarrow j\rho d\rho d\theta$

$$G \propto \int_0^\alpha \int_r^{r+w} \frac{\rho d\rho d\theta}{\rho^2 e^{-2i\theta}} \propto \sin(2\alpha) \log\left(1 + \frac{w}{r}\right)$$

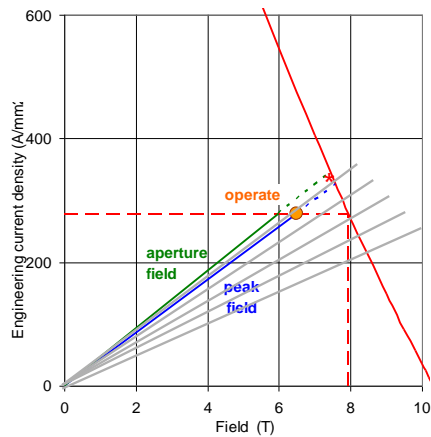
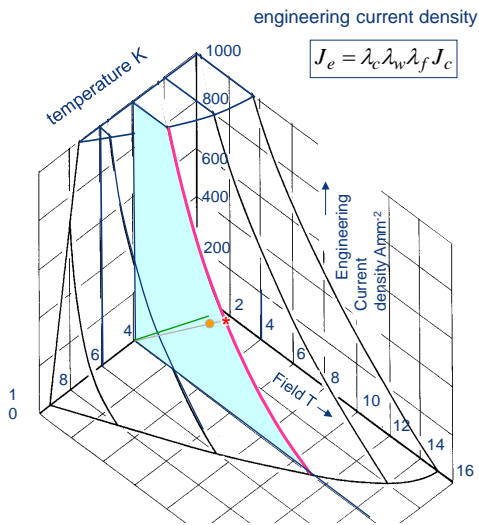
$$G = j\gamma_0 \log\left(1 + \frac{w}{r}\right)$$

$G \propto$ current density
 $G \propto$ coil width w
 G is inversely proportional of the aperture r

Approximate expression of the field



<p><i>In the aperture</i></p> $\begin{Bmatrix} B_r \\ B_\phi \end{Bmatrix} = -\frac{j \mu_0}{\pi} \left\{ (r_i + w) - r_i \right\} 2 \sin \alpha_0 \begin{Bmatrix} \sin \varphi \\ \cos \varphi \end{Bmatrix}$ <p><i>Outside the coil</i></p> $\begin{Bmatrix} B_r \\ B_\phi \end{Bmatrix} = -\frac{j \mu_0}{\pi} \left\{ \frac{(r_i + w)^3 - r_i^3}{3 r^2} \right\} 2 \sin \alpha_0 \begin{Bmatrix} \sin \varphi \\ \cos \varphi \end{Bmatrix}$ <p><i>In the coil</i></p> $\begin{Bmatrix} B_r \\ B_\phi \end{Bmatrix} = -\frac{j \mu_0}{\pi} \left\{ (r_i + w) - r_i + \frac{(r_i^3 - r_i^3)}{3 r^2} \right\} 2 \sin \alpha_0 \begin{Bmatrix} \sin \varphi \\ \cos \varphi \end{Bmatrix}$	<p><i>In the aperture</i></p> $\begin{Bmatrix} B_r \\ B_\phi \end{Bmatrix} = -\frac{j \mu_0}{\pi} \left\{ 4r \ln \left(\frac{r_i + w}{r_i} \right) \right\} 2 \sin(2\alpha_0) \begin{Bmatrix} \sin 2\varphi \\ \cos 2\varphi \end{Bmatrix}$ <p><i>Outside the coil</i></p> $\begin{Bmatrix} B_r \\ B_\phi \end{Bmatrix} = -\frac{j \mu_0}{\pi} \left\{ \frac{(r_i + w)^4 - r_i^4}{r^3} \right\} 2 \sin(2\alpha_0) \begin{Bmatrix} \sin 2\varphi \\ \cos 2\varphi \end{Bmatrix}$ <p><i>In the coil</i></p> $\begin{Bmatrix} B_r \\ B_\phi \end{Bmatrix} = -\frac{j \mu_0}{\pi} \left\{ 4r \ln \left(\frac{r_i + w}{r_i} \right) + \frac{(r^4 - r_i^4)}{r^3} \right\} 2 \sin(2\alpha_0) \begin{Bmatrix} \sin 2\varphi \\ \cos 2\varphi \end{Bmatrix}$
---	---

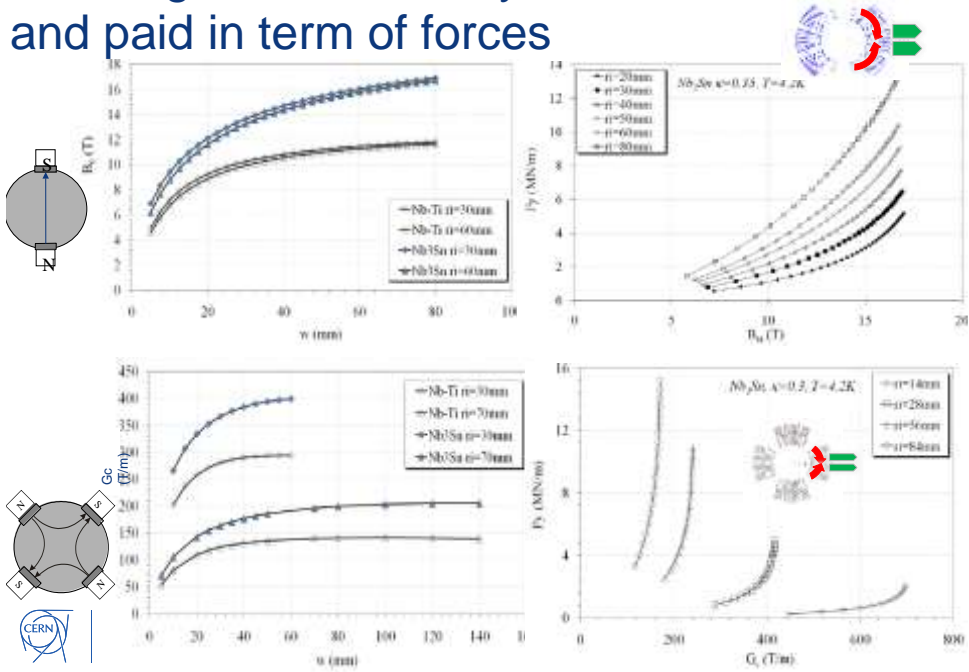


we expect the magnet to go resistive **'quench'** where the peak field load line crosses the critical current line *

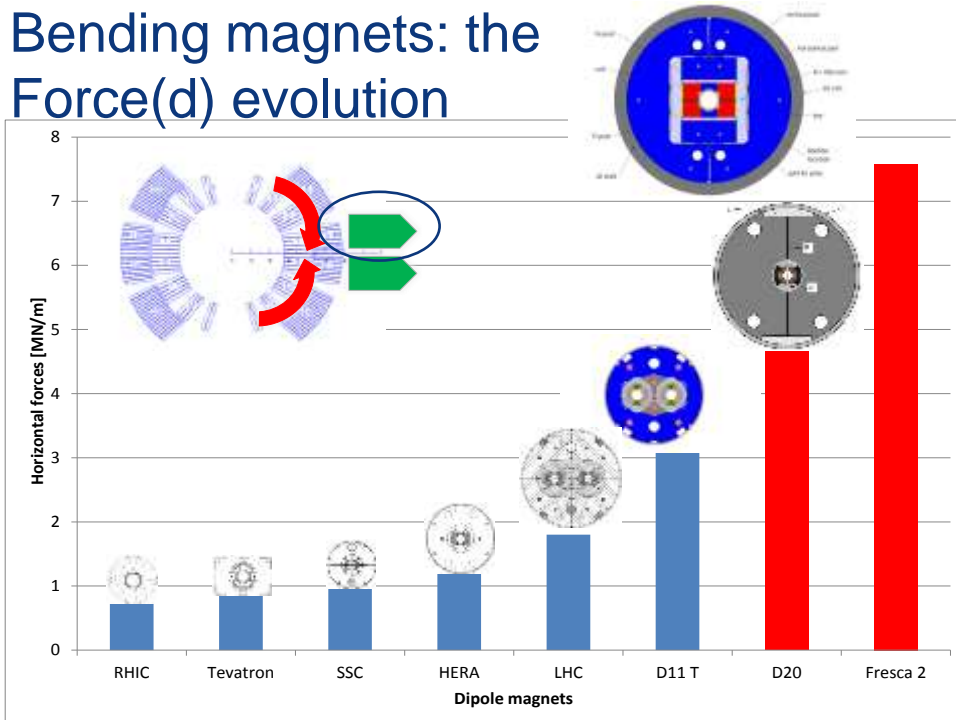
usually back off from this extreme point and operate at ●



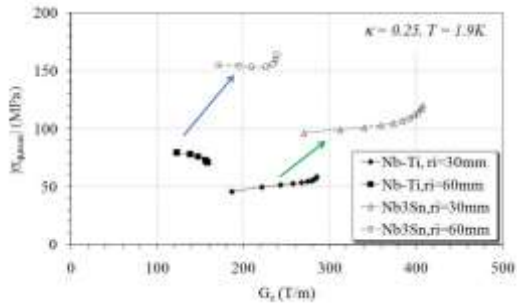
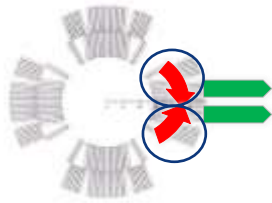
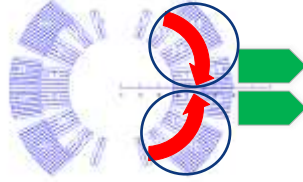
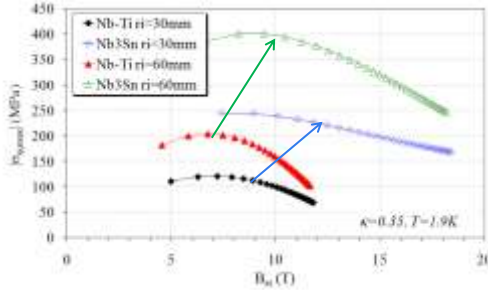
Creating field: limited by the critical surface and paid in term of forces



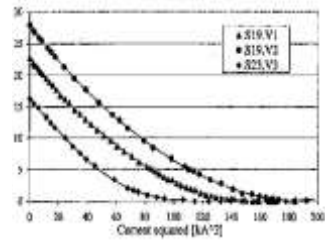
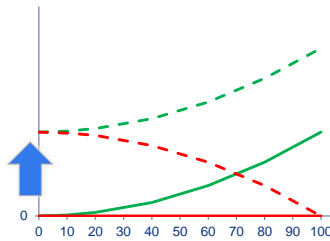
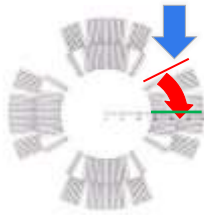
Bending magnets: the Force(d) evolution



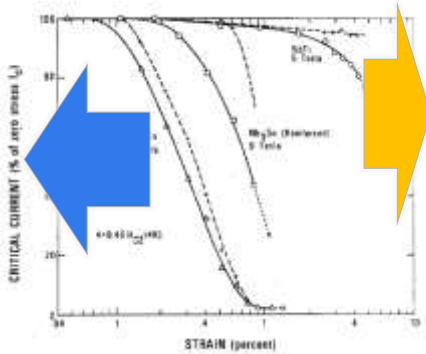
And what about stresses ?



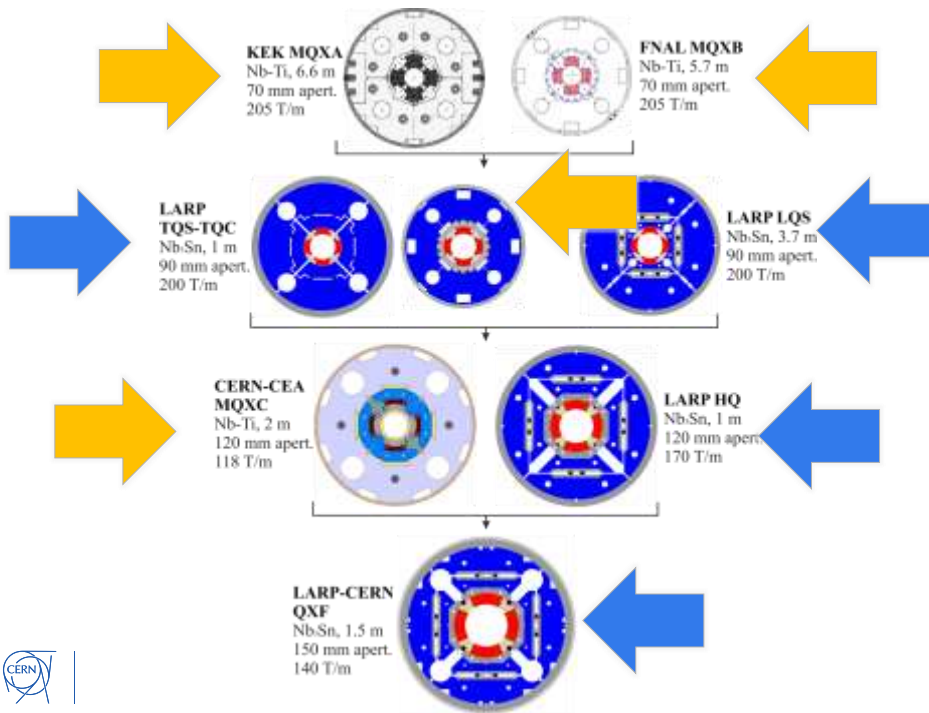
Preventing coil movement: preload



Adding pre-compression during cool down due to differential thermal contraction of components. Mechanical structure and assembly controlled by force



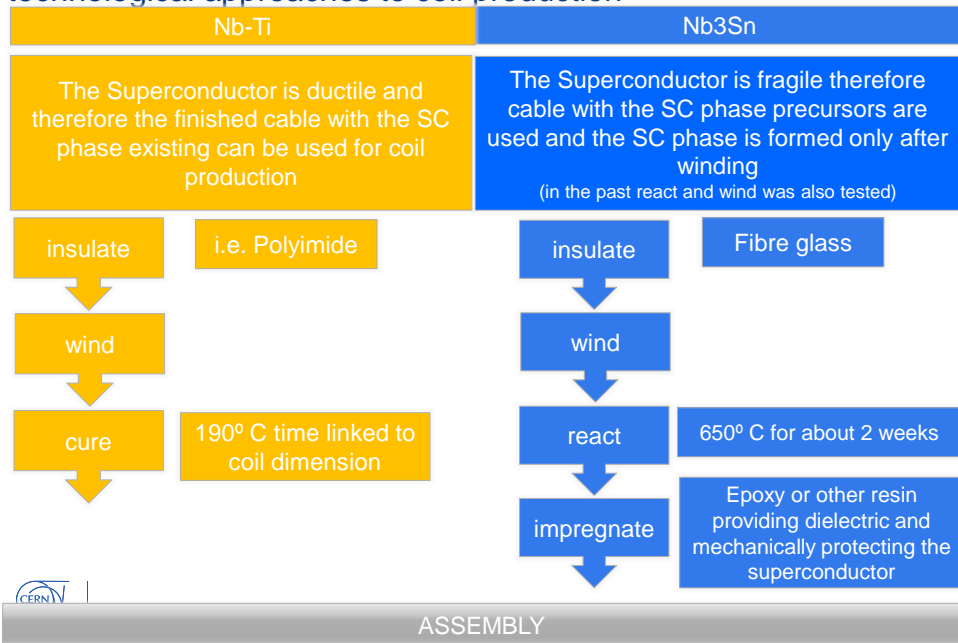
Adding pre-compression at warm during mechanical assembly. Mechanical structure and assembly controlled by displacement



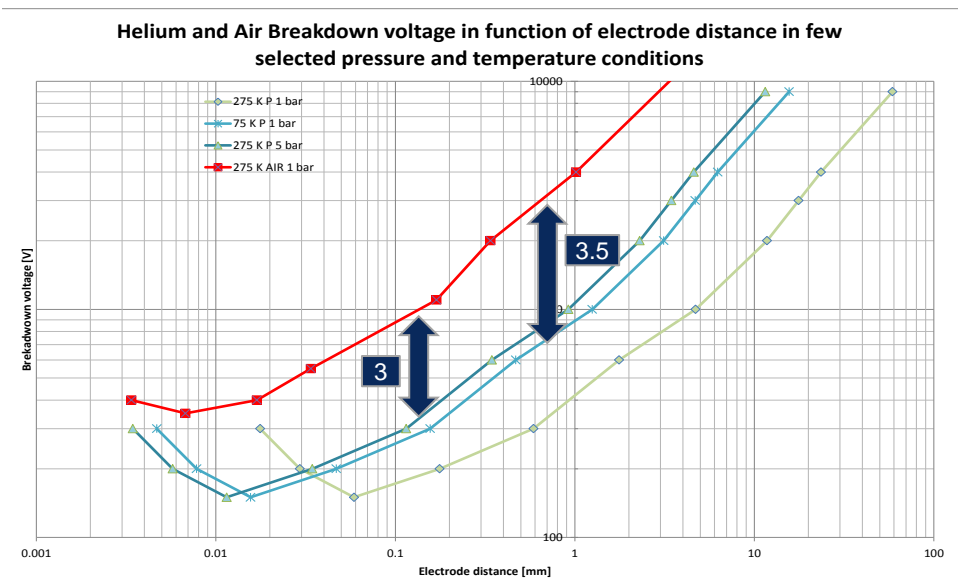
Superconducting magnets an example of technological issue: the insulation



Stress sensitivity, different materials, new problems, new technological approaches to coil production



The environment as dielectric



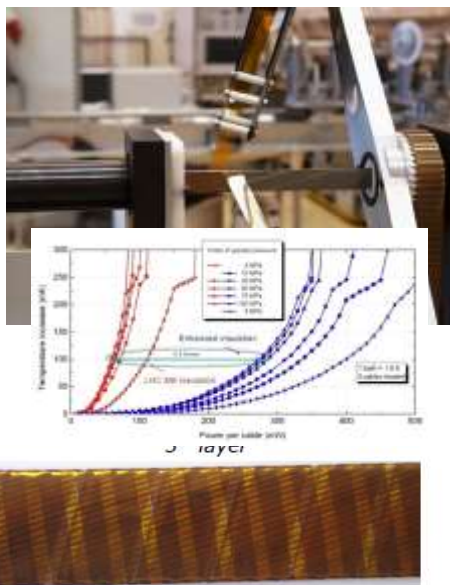
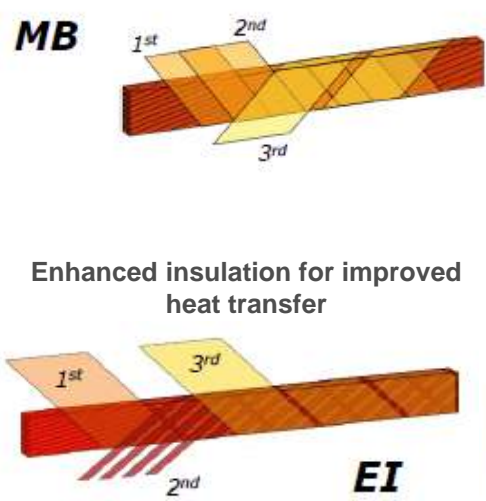
The environment as dielectric

The liquid helium is a very good insulator, but the largest voltages in Sc devices appear during quench. Quench normally create local heating and therefore vaporization of He. Insulation design shall be performed therefore taking as reference gaseous helium

During component fabrication tests are performed in air. Therefore the test voltages shall be a large multiple (i.e. x 5) of the voltages to be withstood in gaseous helium condition

- Sc magnet insulation shall be
- 1) Capable of withstanding few thousands volts in gaseous helium
 - 2) Withstand high stress
 - 3) Working at cryogenic temperature
 - 4) As thin as possible to dilute as low as possible J
 - 5) Provide good heat transfer

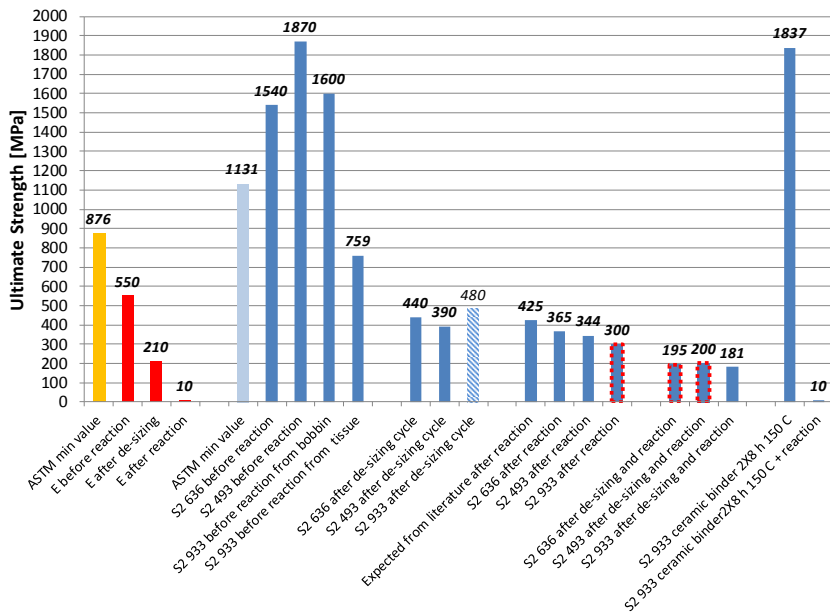
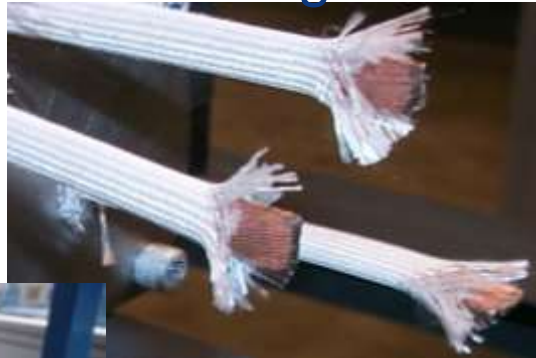
Insulation for Nb-Ti



211

Insulation for Nb₃Sn magnets

- In Nb₃Sn magnets, where cable are reacted at 600-700 °C, the most common insulation is a tape or sleeve of fiber-glass.
- Typically the insulation thickness varies between 70 and 200 μm.

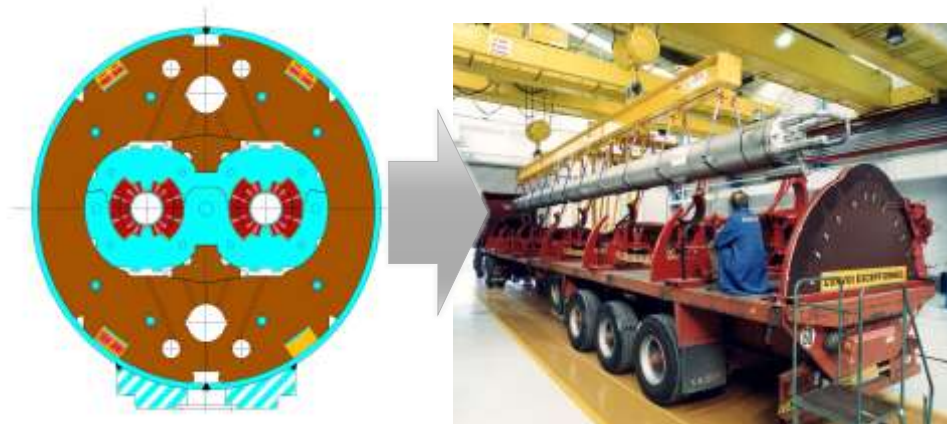


1

Superconducting magnets construction



Example of assembly process: the LHC Nb-Ti main dipole



Coil production I



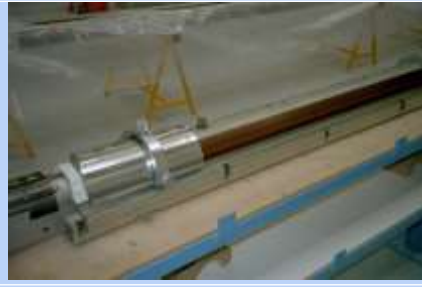
Cable insulation



Coil winding I



Coil winding II



Preparation for curing

Coil production and collaring



Curing press



Ready for collaring



Collaring press



Collared coils ready for cold mass assembly

Cold mass assembly



Introducing collared coils in cold masses



Shell welding

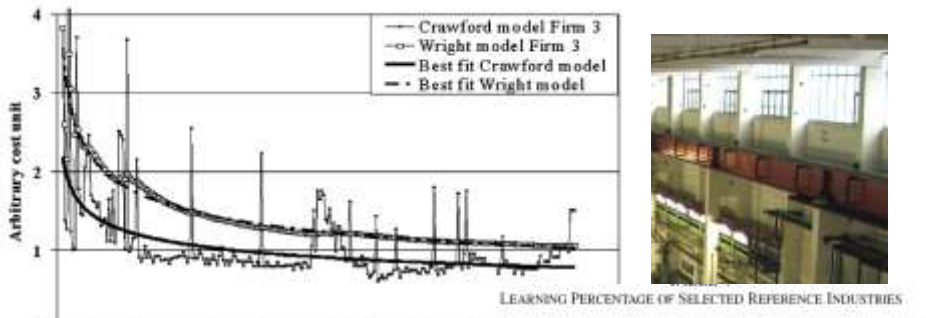


Feet and alignment



Instrumentation completion





LEARNING PERCENTAGE OF SELECTED REFERENCE INDUSTRIES

Industry	L_p
Complex machine tools for new models	75%-85%
Repetitive electrical operations	75%-85%
Shipbuilding	80%-85%
Aerospace	85%
Purchased Parts	85%-88%
Repetitive welding operations	90%
Repetitive electronics manufacturing	90%-95%
Repetitive machining or punch-press operations	90%-95%
Raw materials	93%-96%



TABLE I
LEARNING PERCENTAGE ACCORDING TO CRAWFORD AND WRIGHT MODELS
COLLARED COILS PRODUCTION

Firm	Crawford Model	Wright Model
Firm 1	88%	88%
Firm 2	90%	86%
Firm 3	89%	88%

TABLE II
LEARNING PERCENTAGE ACCORDING TO CRAWFORD AND WRIGHT MODELS
COLD MASS PRODUCTION

Firm	Crawford Model	Wright Model
Firm 1	83%	81%
Firm 2	82%	81%
Firm 3	88%	82%

Thanks you for your attention





www.cern.ch